PHYSICAL REVIEW C VOLUME 43, NUMBER 1 JANUARY 1991

ARTICLES

Integro-differential equation approach. II. Triton and α-particle wave functions, graphical plots

W. Oehm, S. A. Sofianos, and H. Fiedeldey
Physikalisches Institut, Universität Bonn, 5300 Bonn 1, West Germany
and Physics Department, University of South Africa, Pretoria 0001, South Africa

M. Fabre de la Ripelle
Institute de Physique Nucléaire, Université de Paris–Sud, 91406 Orsay, France
and Physics Department, University of South Africa, Pretoria 0001, South Africa
(Received 7 May 1990)

Three- and four-nucleon ground-state wave functions are displayed graphically in coordinate space as well as the Faddeev amplitudes from which they are constructed. In the four-body case only two-particle correlations are taken into account in the integro-differential equation approach, which consequently allows us to make a direct comparison between the Faddeev amplitudes for three and four nucleons and to demonstrate their high degree of similarity in shape. We also investigate the effect of the inclusion of the hypercentral potential in the definition of the (modified) Faddeev amplitudes. It is shown that the Faddeev-type components calculated in the adiabatic approximation are rather similar in shape to those calculated by means of the exact solution of the system of coupled integro-differential equations in two variables. The mixed symmetry component of the Faddeev-type amplitudes show the greatest sensitivity to the number of nucleons, the inclusion of the hypercentral potential, and to the adiabatic approximation.

I. INTRODUCTION

In the first paper[1] of this series of applications of the integro-differential equation approach (IDEA) to three- and four-nucleon bound-state problems, we compared binding energies obtained by solving the two-variable integro-differential equations for central forces with those found by other means of other methods. In particular, we also considered spin-dependent Malfliet-Tjon forces leading to two coupled integro-differential equations. If the local potential acts in all partial waves, we demonstrated that the inclusion of the hypercentral potential in the definition of the Faddeev components both for $A=3$ and 4, which we called the IDEA, results in a considerable improvement in the binding energy as compared to the approximation of the local potential by its S-wave projection (SIDE).[2,3] For such a fully local potential, even in the case of the three-body Faddeev equation, a large system of coupled integro-differential equations in various partial waves must be solved. The IDEA, however, does not require more numerical effort than the treatment of an S-wave projected potential, since the inclusion of the hypercentral potential does not increase the number of coupled equations, although it takes the effect of the higher partial waves in the interacting pair largely into account.[1–3]

This is also true for the four-nucleon system. In that case two-variable integro-differential equations, in both the SIDE and IDEA, only take the two-body correlations exactly into account, but have been shown to give excellent results for the binding energies as compared to, e.g., the essentially exact Green's-function Monte Carlo (GFMC) method.[2,3] In Ref. 1 we demonstrated that all our previous conclusions concerning the SIDE and IDEA for spin-independent forces[2] remain valid for spin-dependent ones. In particular, we found that the interpolated binding energy obtained from the extreme adiabatic approximation (EAA) and the uncoupled adiabatic approximation (UAA) is in good agreement with the result obtained by the exact solution of the integro-differential equations.

However, good agreement of the binding energies does not necessarily mean that the wave functions are also good approximations, as seen from the example of variational methods. It is therefore important that we also compare the wave functions of the adiabatic approximation to the exact solutions.

In this paper we extend our previous calculations of the binding energies and present three-dimensional graphical plots of the Faddeev components and the wave functions of the triton and ^{4}He ground states calculated with MT-V and MT-I/III forces. Our study is in the same spirit as the work on graphical plots of the Faddeev components and the wave functions for the triton presented by Friar *et al.*[4] However, we also treat the four-nucleon system. Since we restrict ourselves to two-body correlations only, which means that our equations remain two-variable equations for any $A \geq 3$, our Faddeev components for $A=4$ cannot completely represent the exact four-nucleon wave function. The exact Faddeev components in this case are obtained by adding the relevant Faddeev-Yakubovsky components which are functions of three variables for S-wave projected potentials, while our Faddeev components depend only on two variables. They have a higher degree of symmetry in the coordinates not referring to the interacting pair defining

the Faddeev component. Consequently, our Schrödinger wave function is also only an approximation of the exact one. This is an unavoidable consequence of the restriction to two-particle correlations only in our approach. It is the price we have to pay for dealing with manageable two-variable integro-differential equations for four and more nucleons, and we have already shown[1] that this price is not too high as far as the binding energies are concerned.

By comparing the Faddeev components obtained by the exact solution of the two-variable integro-differential equations to those found by means of the adiabatic approximation, we can establish whether the adiabatic approximation is not only good for the binding energies, but also for the wave functions, particularly for the four-nucleon system. Another interesting aspect is that our approach allows us to compare the Faddeev components for three- and four-nucleon systems directly, since the latter only include two-particle correlations and therefore only depend on two variables. The considerable improvement resulting from the inclusion of the hypercentral potential in the IDEA as compared to the SIDE also lends considerable interest to a direct comparison of their Faddeev components, to give us an indication of why the IDEA is so successful.

In Sec. II we briefly summarize the formalism which was fully explained in Ref. 1, while in Sec. III the graphical plots of the triton and α-particle Faddeev components and Schrödinger wave functions are presented and discussed, followed by the conclusions in Sec. IV.

II. FORMALISM

In Refs. 1–3 the integro-differential equation approach to the many-body bound system has been reviewed and explained in detail. The three-nucleon system with tensor forces was treated in Ref. 5, while the extension to four nucleons interacting with spin-dependent forces only was given in Ref. 1, the first paper of this series.

To clarify the meaning of the Faddeev components in the four-nucleon case, which will be presented in Sec. III, we recall that in the so-called IDEA we define A-body Faddeev-type components of the wave function $\Psi(\mathbf{x})$, where $\mathbf{x}$ represents all the particle coordinates and $\mathbf{r}_{ij}=\mathbf{r}_i-\mathbf{r}_j$ with $\mathbf{r}_i$ being the coordinate of particle i, by

$$\left[T+\frac{A(A-1)}{2}V_0(r)-E\right]\psi_{ij}(\mathbf{x}) = -[V(r_{ij})-V_0(r)]\psi(\mathbf{x}) . \quad (2.1)$$

Here the hypercentral potential $V_0(r)$ represents the first term of the potential harmonic expansion of the interaction. For S-wave projected two-body potentials, $V_0(r)$ is set equal to zero and we revert to the SIDE.[1]

For pure Wigner forces like the MT-V potentials, Eq. (2.1) reduces to a single integro-differential equation and, for spin-dependent central forces like the MT-I/III potentials, to a set of two coupled integro-differential equations in two variables, namely, the hyperradius given by $r^2=2/A\sum r_{ij}^2$ and the coordinate $z=2r_{ij}^2\ r^{-2}-1$ for three- and four-nucleon ground states. In terms of the coordinates z and r, the even Faddeev-type component $\psi_{ij}^{+}(\mathbf{x},s,t)$ can, after projection on the $\mathbf{r}_{ij}$ space, be written for three bodies as

$$\langle \mathbf{r}_{ij}|\psi_{ij}^{+}(\mathbf{x},s,t)\rangle = r^{-5/2}Y_{00}(\omega_{ij}) \times[|A\rangle P_0^s(z,r)+|A'_{ij}\rangle P_0^{s'}(z,r)] , \quad (2.2)$$

where s and t refer to spin and isospin, ω_{ij} to the angular coordinates of $\mathbf{r}_{ij}$, $|A\rangle$ and $|A'_{ij}\rangle$ to the fully and mixed antisymmetric spin and isospin state, respectively, and the fully symmetric (S) and mixed symmetric (S') spatial components are denoted by P_0^s and $P_0^{s'}$. For four bodies we have

$$\langle \mathbf{r}_{ij}|\psi_{ij}^{+}(\mathbf{x},s,t)\rangle = r^{-4}Y_{00}(\omega_{ij}) \times[|A\rangle P_0^s(z,r)+|A'_{ij}\rangle P_0^{s'}(z,r)] , \quad (2.3)$$

in the approximation where only two-particle correlations are taken into account. This has the consequence that only two variables z and r occur in Eq. (2.3).

In the exact four-body theory, the Faddeev components consist of a sum of Faddeev-Yakubovsky components,[6,7] which in the simplest case of S-wave projected potentials are functions of three variables each. It is therefore obvious that each set (z,r) in the Faddeev component of Eq. (2.3) relates to different combinations of three variables in each of the Faddeev-Yakubovsky components, which together add up to this Faddeev component.

The Schrödinger wave function which we obtain by summing up the six four-body Faddeev components, represented by Eq. (2.6), is therefore not the exact Schrödinger wave function. As mentioned above, it only takes the two-particle correlations into account and neglects all higher-order correlations. Consequently, both the Faddeev components and Schrödinger wave function retain a three-body character for the four-body system (and for $A>4$) in our approach. We can therefore easily compare Faddeev components and Schrödinger wave functions for three- and four-nucleon systems directly.

The Schrödinger wave function Ψ for three nucleons can be written as a sum of its three Faddeev components and expressed in the well-known form

$$\Psi=|A\rangle\psi+|A'_{12}\rangle\phi_1+|S'_{12}\phi_2 , \quad (2.4)$$

where the spin-isospin states are given in Ref. 1, and representing the Faddeev-type components ψ_{ij} by the functions $P_0^s(ij)$ and $P_0^{s'}(ij)$, the spatial wave functions may be written as

$$\begin{aligned}\psi&=\frac{r^{-5/2}}{2\sqrt{\pi}}[P_0^s(12)+P_0^s(23)+P_0^s(31)] ,\\ \phi_1&=\frac{r^{-5/2}}{2\sqrt{\pi}}[P_0^{s'}(12)-\tfrac{1}{2}P_0^{s'}(23)-\tfrac{1}{2}P_0^{s'}(31)] ,\\ \phi_2&=\frac{\sqrt{3}}{2}\frac{r^{-5/2}}{2\sqrt{\pi}}[P_0^{s'}(31)-P_0^{s'}(23)] .\end{aligned} \quad (2.5)$$

TABLE I. Three-nucleon binding energies in MeV and S and S' probabilities in %.

Force	Method	Exact solution E	Exact solution $P(S)$	Exact solution $P(S')$	EAA E	EAA $P(S)$	EAA $P(S')$	Faddeev E
MT-V	SIDE	7.54	100		7.83	100		7.541 (Ref. 4)
MT-V	IDEA	7.68	100		8.03	100		7.736 (Ref. 8)
MT-I/III	SIDE	8.54	98.05	1.95	8.99	99.29	0.71	8.536 (Ref. 4)
MT-I/III	IDEA	8.86	97.14	2.86	9.40	97.65	2.35	

For the four-nucleon system, the Schrödinger wave function is of the same form as in Eq. (2.4), but

$$\psi=\frac{r^{-4}}{2\sqrt{\pi}}\sum_{i<j\le 4}P_0^s(ij)\ ,$$

$$\phi_1=\frac{r^{-4}}{2\sqrt{\pi}}\{P_0^{s'}(12)+P_0^{s'}(34) -\tfrac{1}{2}[P_0^{s'}(23)+P_0^{s'}31) +P_0^{s'}(24)+P_0^{s'}(41)]\}\ , \tag{2.6}$$

$$\phi_2=\frac{\sqrt{3}}{2}\frac{r^{-4}}{2\sqrt{\pi}}[P_0^{s'}(31)+P_0^{s'}(24)-P_0^{s'}(23)-P_0^{s'}(41)]\ .$$

This result can be derived from the definition of the Schrödinger wave function Ψ as

$$\Psi(\mathbf{x})=\sum_{i<j\le A}\psi_{ij}(\mathbf{x})\ , \tag{2.7}$$

or, alternatively, by substituting $[P_0(ij)+P_0(kl)]$ for $P_0(ij)$ in Eq. (2.5), both for the S and S' components, and writing r^{-4} instead of $r^{-5/2}$. Here $(ijkl)$ represents any cyclic permutation of (1234).

In Ref. 1 the projection of the total wave function Ψ on the $\mathbf{r}_{ij}$ space was also derived. For three-nucleon systems it is given by

$$\langle \mathbf{r}_{ij}|\Psi^+(\mathbf{x},s,t)\rangle=r^{-5/2}Y_{00}(\omega_{ij}) \times[|A\rangle\Pi_0^s(z,r)+|A'_{ij}\rangle\Pi_0^{s'}(z,r)]\ , \tag{2.8}$$

where

$$\Pi_0^s(z,r)=P_0^s(z,r)+\frac{2}{[3(1-z^2)]^{1/2}}\int_{z_-}^{z_+}P_0^s(z',r)dz'\ , \tag{2.9}$$

$$\Pi_0^{s'}(z,r)=P_0^{s'}(z,r)-\frac{1}{[3(1-z^2)]^{1/2}}\int_{z_-}^{z_+}P_0^{s'}(z',r)dz'\ , \tag{2.10}$$

with $z_\pm=\frac{1}{2}\{-z\pm[3(1-z^2)]^{1/2}\}$. For four-nucleon systems we find

$$\langle \mathbf{r}_{ij}|\psi^+(\mathbf{x},s,t)\rangle=r^{-4}Y_{00}(\omega_{ij}) \times[|A\rangle\Pi_0^s(z,r)+|A'_{ij}\rangle\Pi_0^{s'}(z,r)]\ , \tag{2.11}$$

where $\Pi_0(z,r)$ for S and S' are now given by more complicated expressions derived in Ref. 1. By means of Eq. (2.1) and (2.8)–(11), the coupled system of two integro-differential equations for $P_0^s(z,r)$ and $P_0^{s'}(z,r)$ has been derived in Ref. 1, for both the three- and four-nucleon systems. They can be solved exactly as two-variable equations or by means of the adiabatic approximation as described in Ref. 1.

III. RESULTS AND GRAPHICAL PLOTS

The numerical methods employed to solve the (coupled) integro-differential equation(s) for the spin-(in)dependent MT-V (Ref. 8) and MT-I/III (Ref. 9) central potentials have been described in Ref. 1, as well as those used for the solution of the corresponding extreme adiabatic approximation (EAA) and uncoupled adiabatic approximation (UAA). These methods have been extended to larger nuclei, like the 16-fermion system[10] interacting by means of the MT-V force, with no increase in the numerical effort required. In fact, it has been found that the difference between the EAA and UAA, which provide variational upper and lower bounds to the binding energy of the A-body system, decreases rapidly with in-

TABLE II. Same as in Table I, but for four nucleons.

Force	Method	Exact solution E	Exact solution $P(S)$	Exact solution $P(S')$	EAA E	EAA $P(S)$	EAA $P(S')$	Other methods E
MT-V	SIDE	28.47	100		28.91	100		
MT-V	IDEA	29.37	100		29.91	100		
MT-I/III	SIDE	29.74	99.27	0.73	30.45	99.20	0.80	30.36 (Ref. 11) 29.6 (Ref. 12)
MT-I/III	IDEA	31.02	98.51	1.49	31.78	98.60	1.40	

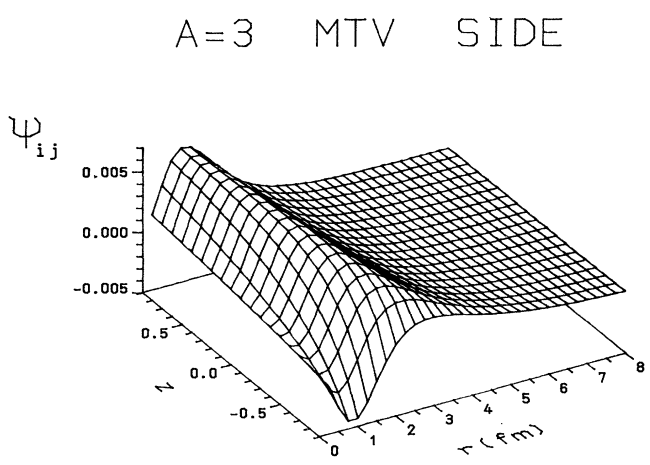

FIG. 1. Exact three-nucleon Faddeev amplitude ψ_{ij} for the MT-V potential in the case of the SIDE, displayed in terms of the coordinates r and z.

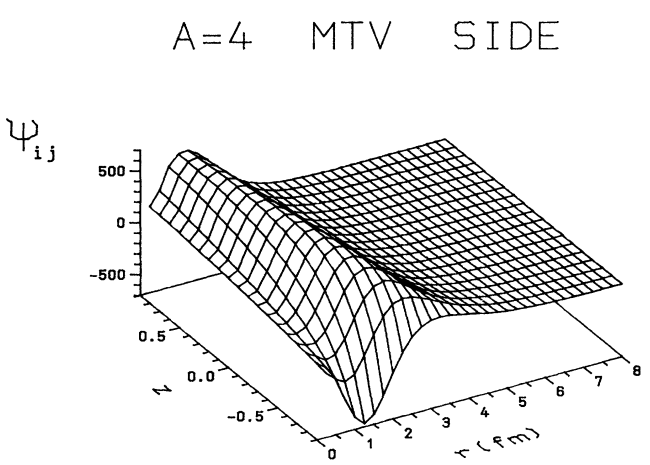

FIG. 3. Exact four-nucleon Faddeev amplitude ψ_{ij} for the MT-V potential in the case of the SIDE, displayed in terms of the coordinates r and z. Note that the values of the z axis are enlarged by a factor of 10^6.

creasing A. The very simple EAA therefore rapidly becomes rather accurate for larger values of A. In this paper, however, we restrict ourselves to the triton and α particle and to the MT-V and MT-I/III forces, but also consider the case, as in Ref. 1, where these potentials are not only treated as S-wave projected potentials, but also are assumed to act in all partial waves like a fully local potential. In the latter case we solve Eq. (2.1), including the hypercentral potential $V_0(r)$, in our definition of the Faddeev components. We call this approximation the IDEA. If $V_0(r)$ is canceled in Eq. (2.1), we revert to the SIDE for S-wave projected potentials. The binding energies calculated for the triton and ^{4}He in the IDEA and SIDE with these forces have already been given in Ref. 1. Some of them are again represented here together with the probabilities $P(S)$ and $P(S')$ of the fully and mixed symmetric components for the MT-I/III potential in Tables I and II. For completeness we also present binding energies calculated by alternative methods.

In order to solve the coupled system of integro-differential equations in $P_0^s(z,r)$ and $P_0^{s'}(z,r)$, these functions have been expanded in terms of Hermite splines. The resulting system of algebraic equations has then been solved by means of the orthogonal collocation technique.[13] Writing

$$P_0(z,r)=\frac{e^{-\kappa r}p_0(z,r)}{(1-z)^{\alpha}(1+z)^{\beta}}\ , \tag{3.1}$$

with $E=\hbar^2\kappa^2/m$, $\alpha=(D-5)/2$, and $\beta=\frac{1}{2}$, where $D=3(A-1)$, the function $p_0(z,r)$ is represented by

$$p_0(z,r)=\sum_{m}^{2I_z}\sum_{n}^{2I_r} c_{mn}s_m(z)s_n(r)\ , \tag{3.2}$$

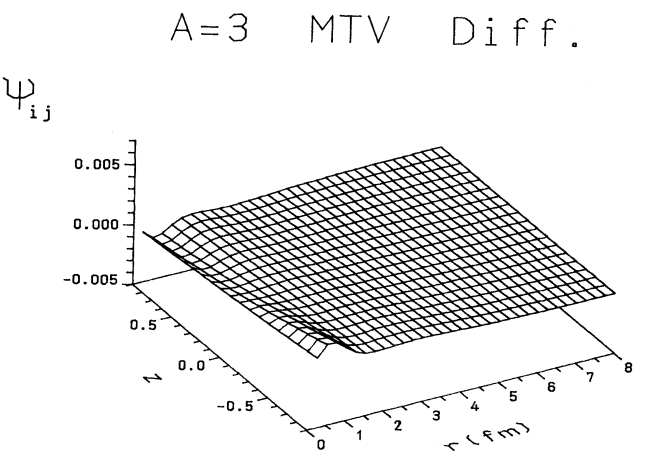

FIG. 2. Difference between the IDEA and SIDE for the exact three-nucleon Faddeev amplitude ψ_{ij} for the MT-V potential, displayed in terms of the coordinates r and z.

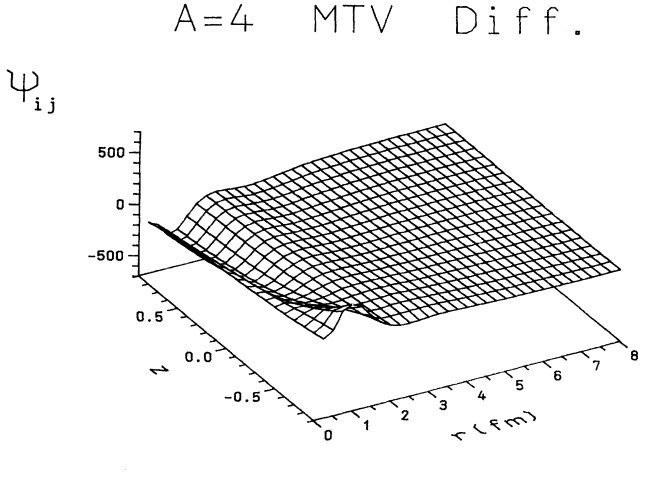

FIG. 4. Difference between the IDEA and SIDE for the exact four-nucleon Faddeev amplitude ψ_{ij} for the MT-V potential, displayed in terms of the coordinates r and z. Note that the values of the z axis are enlarged by a factor of 10^6.

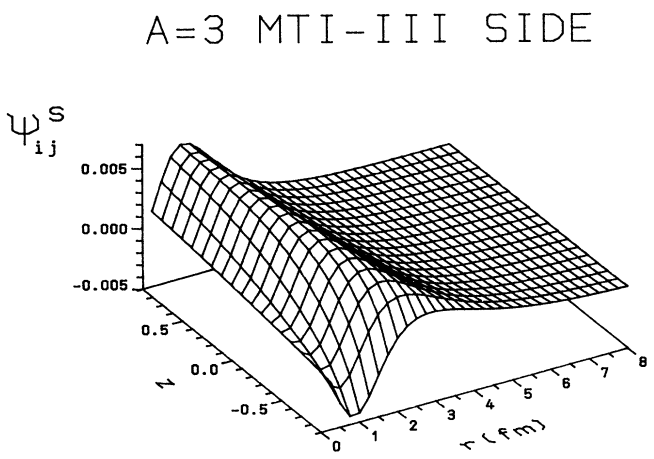

FIG. 5. Exact three-nucleon Faddeev amplitude ψ^s_{ij} for the MT-I/III potential in the case of the SIDE, displayed in terms of the coordinates r and z.

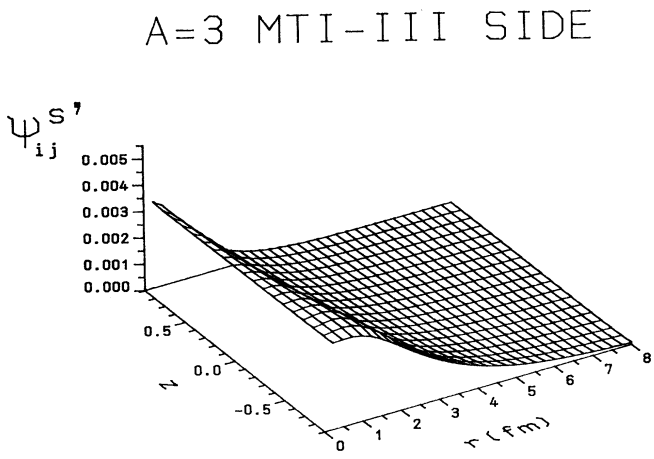

FIG. 7. Exact three-nucleon Faddeev amplitude $\psi^{s'}_{ij}$ for the MT-I/III potential in the case of the SIDE, displayed in terms of the coordinates r and z.

where the $s_m(z)$ and $s_n(r)$ are Hermite splines. The Faddeev-type components and wave-function components given in Sec. II are finally expressed in terms of Eqs. (3.1) and (3.2), using $I_z=18$ subdivisions for the coordinate z and $I_r=13$ for the hyperradius r in the case $A=3$, and $I_z=16$ and $I_r=15$ for the four-nucleon system. In contrast to the exact solution, the EAA results have been obtained by the use of B splines as described in Ref. 2.

It has already been explained by Friar *et al.*[4] for the three-nucleon problem that the Faddeev amplitude ψ_{ij} can have a quite different behavior than the total Schrödinger wave function Ψ. The completely symmetrical ground-state wave function for a local potential can be chosen to be positive definite. However, the Faddeev amplitudes can have nodes, due to the non-Hermitian character of the "Hamiltonian" of the Faddeev equation, even though the three Faddeev components add up to a positive-definite Schrödinger wave function. Another important difference is that the Faddeev amplitude generated by an S-wave projected two-body potential only contains an S-wave relative orbital angular momentum, while the total wave function incorporates all partial waves, which are induced through the other Faddeev components obtained by permutations of the particles.

For the S-wave projected MT-V and MT-I/III potentials, the Faddeev amplitude ψ_{ij} and total Schrödinger wave function have already been plotted by Friar *et al.*[4] Since our Faddeev amplitudes for three-nucleon systems and the SIDE are identical to those of Friar *et al.*, we only repeat them here for comparison purposes between the SIDE, IDEA, and the EAA, and because we find it more convenient to plot them as functions of the variables r and z instead of the Jacobi coordinates x and y

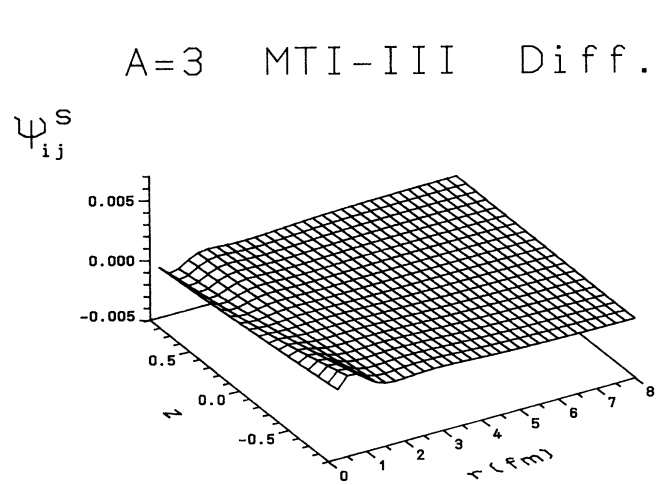

FIG. 6. Difference between the IDEA and SIDE for the exact three-nucleon Faddeev amplitude ψ^s_{ij} for the MT-I/III potential, displayed in terms of the coordinates r and z.

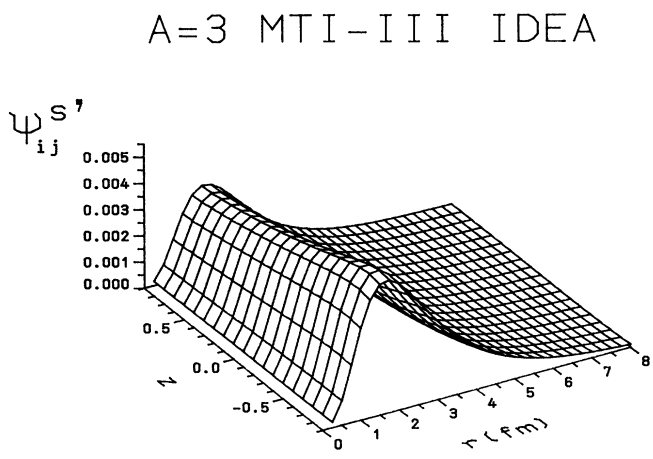

FIG. 8. Exact three-nucleon Faddeev amplitude $\psi^{s'}_{ij}$ for the MT-I/III potential in the case of the IDEA, displayed in terms of the coordinates r and z.

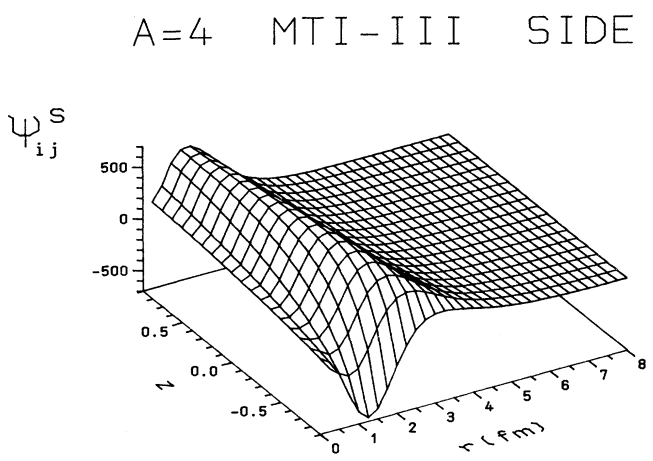

FIG. 9. Exact four-nucleon Faddeev amplitude ψ^s_{ij} for the MT-I/III potential in the case of the SIDE, displayed in terms of the coordinates r and z. Note that the values of the z axis are enlarged by a factor of 10^6.

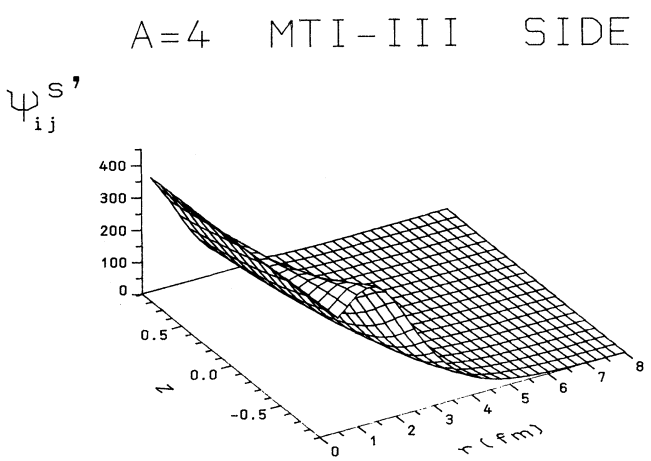

FIG. 11. Exact four-nucleon Faddeev amplitude $\psi^{s'}_{ij}$ for the MT-I/III potential in the case of the SIDE, displayed in terms of the coordinates r and z. Note that the values of the z axis are enlarged by a factor of 10^6.

employed by these authors.

Another major reason for plotting them is, of course, to compare the Faddeev-type components $\psi_{ij}(z,r)$ for the triton and α particle, which in our case can easily be performed as previously explained, because of our restriction to two-particle correlations only in these amplitudes.

In Fig. 1 we plot the exact $\psi_{ij}(r,z)$ ($A=3$) for the MT-V potential in the SIDE and display the difference between the IDEA and SIDE in this case in Fig. 2. It is clear from these figures that both amplitudes are very similar, which is not unexpected in view of the rather small increase in the binding energy of about 0.14 MeV between the IDEA, due to the inclusion of $V_0(r)$ in the definition of its Faddeev components, and the SIDE. As in the plots of Friar *et al.*[4], our amplitudes $\psi_{ij}(z,r)$ assume positive and negative values. Most intriguing, however, is the similarity in the shape of ψ_{ij} for $A=3$ and 4, particularly for the SIDE, but also for the IDEA, although of course the normalizations differ. This can easily be confirmed from our plots of $\psi_{ij}(z,r)$ in Figs. 3 and 4. We also note that the relatively small difference between the binding energies in the IDEA and SIDE for $A=4$ of about 0.9 MeV corresponds to very similar shapes of the $\psi_{ij}(z,r)$. In Figs. 5–8 we compare our exact amplitudes $\psi_{ij}(z,r)$ for $A=3$ and the MT-I/III force, which means that we plot $\psi^s_{ij}(z,r)$ and $\psi^{s'}_{ij}(z,r)$ for both the SIDE and IDEA. For the SIDE again our results are identical to those of Friar *et al.*,[4] except that we employ the coordinates z and r instead of Jacobi coordinates. In this case, however, comparison between the $\psi^{s'}_{ij}(z,r)$ for the SIDE and IDEA shows a striking difference in shape, while for

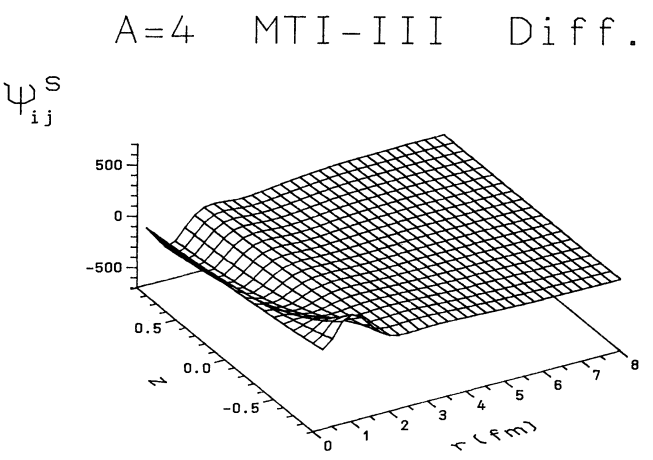

FIG. 10. Difference between the IDEA and SIDE for the exact four-nucleon Faddeev amplitude ψ^s_{ij} for the MT-I/III potential, displayed in terms of the coordinates r and z. Note that the values of the z axis are enlarged by a factor of 10^6.

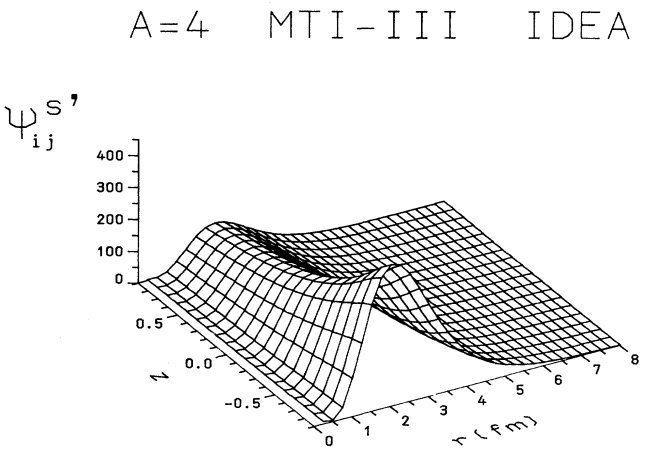

FIG. 12. Exact four-nucleon Faddeev amplitude $\psi^{s'}_{ij}$ for the MT-I/III potential in the case of the IDEA, displayed in terms of the coordinates r and z. Note that the values of the z axis are enlarged by a factor of 10^6.

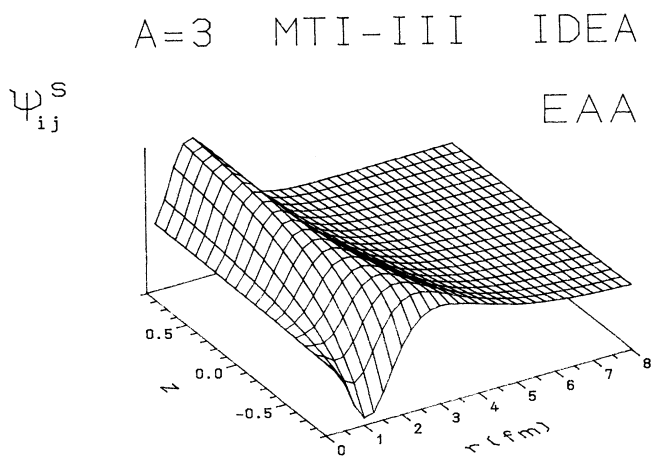

FIG. 13. Three-nucleon Faddeev amplitude ψ^s_{ij} calculated in the extreme adiabatic approximation for the MT-I/III potential in the case of the IDEA, displayed in terms of the coordinates r and z.

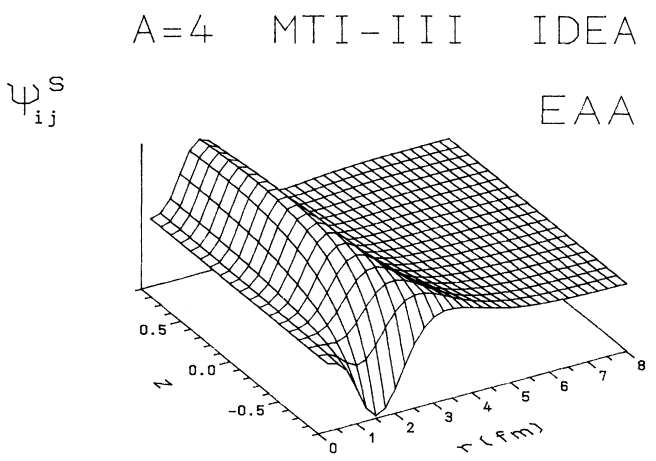

FIG. 15. Four-nucleon Faddeev amplitude ψ^s_{ij} calculated in the extreme adiabatic approximation for the MT-I/III potential in the case of the IDEA, displayed in terms of the coordinates r and z.

$\psi^s_{ij}(z,r)$ the shapes are again very similar. For this reason we again plot the difference between the IDEA and SIDE for $\psi^s_{ij}(z,r)$, while $\psi^{s'}_{ij}(z,r)$ itself is displayed not only for the SIDE, but also for the IDEA. The $\psi^{s'}_{ij}(z,r)$ for the IDEA is far less smooth than for the SIDE, which is in accordance with the difference of about 0.32 MeV in the binding energies. Going from three to four nucleons, we have plotted $\psi^s_{ij}(z,r)$ and $\psi^{s'}_{ij}(z,r)$ for $A=4$ and for the SIDE and IDEA in Figs. 9–12. In agreement with our previous results for the MT-V potential, the $\psi^s_{ij}(z,r)$ are quite similar for the SIDE and IDEA and $A=4$ (see Figs. 9 and 10). For $\psi^{s'}_{ij}(z,r)$ again, as for $A=3$, there is striking difference between the SIDE and IDEA, which is not unexpected since in this case the difference between the binding energies amounts to about 1.3 MeV. Comparing Figs. 7 and 11, we now find that, even in the SIDE, $\psi^{s'}_{ij}(z,r)$ is not as smoothly varying as for $A=3$. This is also true for the IDEA. The major point of interest of these plots is therefore the relatively high degree of sensitivity the $\psi^{s'}_{ij}$ amplitude shows as to whether $V_0(r)$ is included in its definition or not. It is also correlated to a larger degree of sensitivity of the binding energies to the presence of $V_0(r)$ in the case of the MT-I/III potential than for the MT-V potential.

In Figs. 13–16 the same plots as in Figs. 5–12 are repeated for the MT-I/III force and IDEA, but now all the Faddeev-type components have been calculated in the extreme adiabatic approximation. Our purpose is to demonstrate the surprising fact that the EAA already provides us with Faddeev amplitudes which are quite

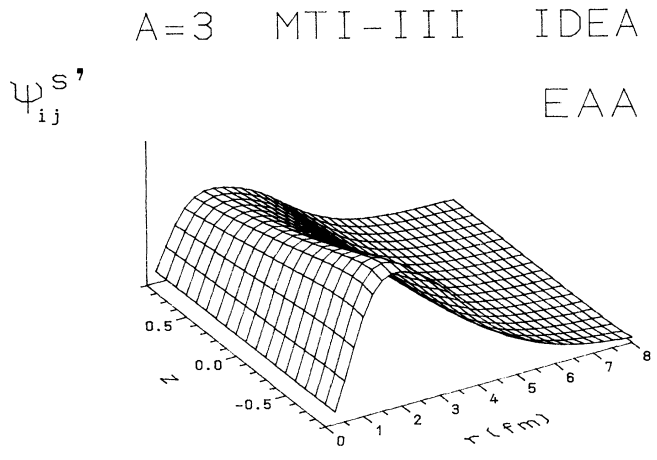

FIG. 14. Three-nucleon Faddeev amplitude $\psi^{s'}_{ij}$ calculated in the extreme adiabatic approximation for the MT-I/III potential in the case of the IDEA, displayed in terms of the coordinates r and z.

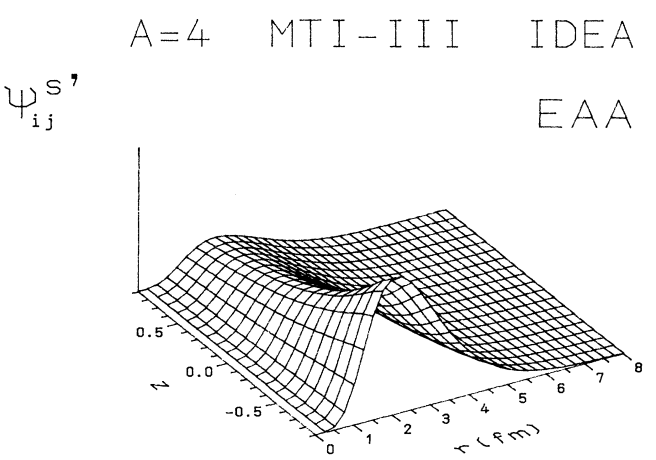

FIG. 16. Four-nucleon Faddeev amplitude $\psi^{s'}_{ij}$ calculated in the extreme adiabatic approximation for the MT-I/III potential in the case of the IDEA, displayed in terms of the coordinates r and z.

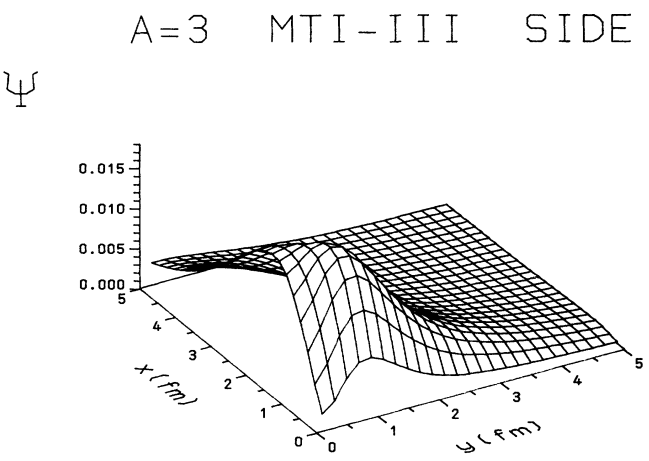

FIG. 17. Exact three-body wave-function component ψ for the MT-I/III potential in the case of the SIDE, displayed in terms of the coordinates x and y.

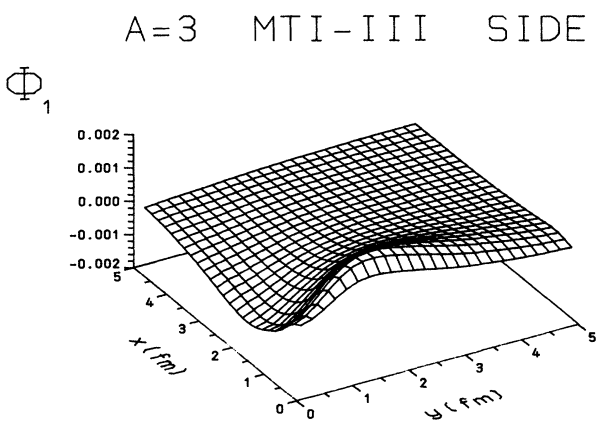

FIG. 19. Exact three-body wave-function component ϕ_1 for the MT-I/III potential in the case of the SIDE, displayed in terms of the coordinates x and y.

near to the exact ones. This is, of course, even more obvious for the UAA, which produces binding energies much closer to the exact ones than the EAA (see Tables I and II). This can also be seen from the interpolation formula $E_I = E^{\mathrm{UAA}} + 0.2(E^{\mathrm{EAA}} - E^{\mathrm{UAA}})$, whose accuracy was demonstrated in Ref. 1. Comparison of Figs. 5, 6, and 13 shows that for three nucleons the EAA and exact calculations produce very similar results for $\psi^S_{ij}(z,r)$ in the IDEA. However, even the shapes of the $\psi^{S'}_{ij}(z,r)$ are quite similar, although to a lesser extent, as can be seen by comparing Figs. 8 and 14. Such comparisons can also be made between the exact Faddeev amplitudes for S and S' states and those obtained in the EAA for four nucleons by comparing Figs. 9 and 10 to Fig. 15 and Fig. 12 to Fig. 16. Once again the similarities of the shapes even for $\psi^{S'}_{ij}(z,r)$ are striking, although for $A=4$ the exact binding energy differs by 0.76 MeV from the one obtained in the EAA. In fact, in all these cases the largest deviation occurs in the S' state for three nucleons. This is consistent with the observation that the EAA improves its accuracy with increasing A. From these plots the conclusion is inescapable that the EAA (and, of course, this holds even more for the UAA) not only provides good estimates of the exact binding energies, but also of the wave functions, for both the three- and four-nucleon systems. In the latter case we again mention that only two-particle correlations are included in our Faddeev-type amplitudes.

We now present plots for the full Schrödinger wave function for some cases. In these plots we use the Jacobi coordinates x and y like Friar *et al.*[4] for the triton. Furthermore, we present the Schrödinger wave function for ^{4}He using Jacobi coordinates, but remind the reader that in this case our wave function is a simplified one, consisting of six Faddeev amplitudes, which only take two-particle correlations into account. As in all previous calculations for the binding energy, we have also neglected the Coulomb force in ^{4}He.

In Fig. 17 we plot the component ψ of the total wave

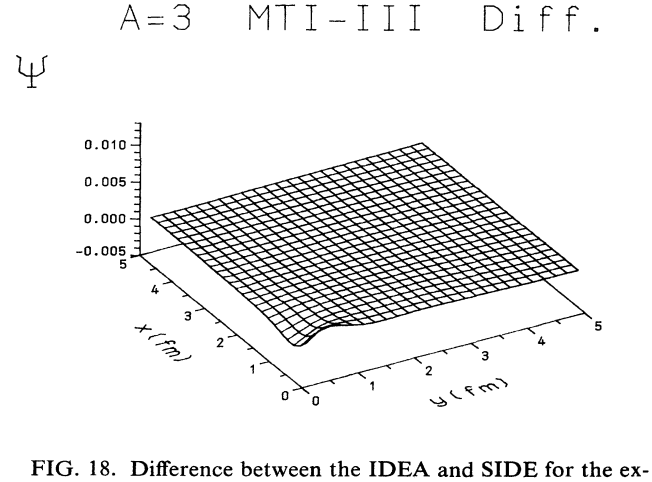

FIG. 18. Difference between the IDEA and SIDE for the exact three-body wave-function component ψ for the MT-I/III potential, displayed in terms of the coordinates x and y.

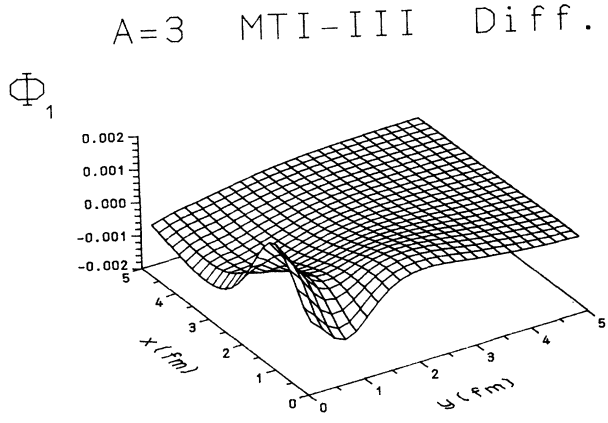

FIG. 20. Difference between the IDEA and SIDE for the exact three-body wave-function component ϕ_1 for the MT-I/III potential, displayed in terms of the coordinates x and y.

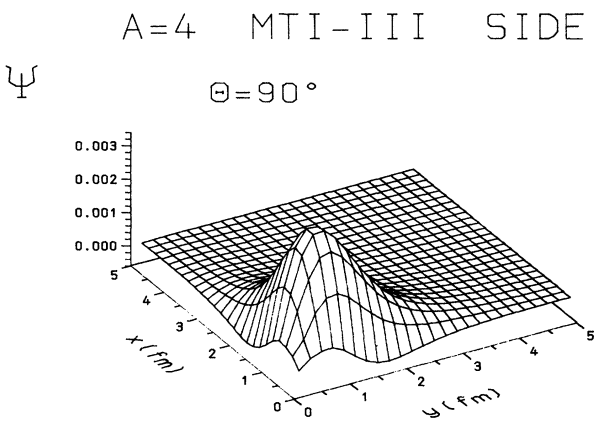

FIG. 21. Exact four-body wave-function component ψ for the MT-I/III potential in the case of the SIDE, displayed in terms of the coordinates x and y.

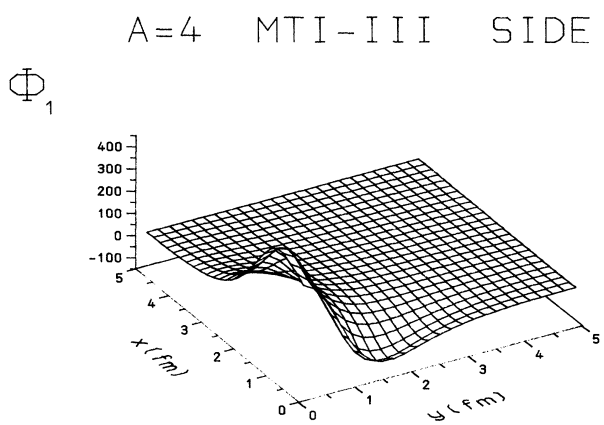

FIG. 23. Exact four-body wave-function component ϕ_1 for the MT-I/III potential in the case of the SIDE, displayed in terms of the coordinates x and y. Note that the values of the z axis are enlarged by a factor of 10^6.

function Ψ in the SIDE for $A=3$, as defined in Eqs. (2.4) and (2.5), in the Jacobi coordinates x and y with $\theta=90°$. x indicates the distance between the particles i and j, y the distance of the third particle k to the center of mass of the two-particle system (ij), and θ the angle between the corresponding vectors **x** and **y**. In Fig. 18 we show the difference for ψ between the IDEA and SIDE, while the wave component ϕ_1 is plotted in Figs. 19 and 20, respectively. The component ϕ_2 vanishes for this configuration, i.e., $\theta=90°$. For the SIDE our wave components ψ and ϕ_1 are identical to those plotted by Friar *et al.*[4] for the same configuration of the trinucleon system and MT-I/III potential, since our integro-differential equations reduce to the Faddeev equations in this case. From Fig. 18 we conclude that, as for the ψ_{ij}^s, the ψ are nearly identical for the SIDE and IDEA. However, corresponding to the difference between the $\psi_{ij}^{s'}$ for the SIDE and IDEA, we find a similar difference in ϕ_1 from Fig. 20, which is of course not surprising

We now turn our attention to the corresponding Schrödinger wave components of ^{4}He for the MT-I/III potential and present plots for rectangular configurations of the four particles, where x and y denote the length of the sides (Figs. 21–26). Now it is not possible anymore to make direct comparisons between the Schrödinger wave components of the triton and ^{4}He in view of the difference between the number of nucleons. Even in our approximation, which only takes two-particle correlations into account, we cannot, of course, construct three- and four-particle configurations, which are directly comparable, as was possible for the Faddeev-type components.

We therefore restrict ourselves here to an internal comparison between the four-nucleon wave-function components in the SIDE and IDEA. From Figs. 21 and 22 we see again how similar ψ is for the SIDE and IDEA, which also holds true for the amplitude ϕ_2 displayed in Figs. 25 and 26, while Figs. 23 and 24 show that there is a

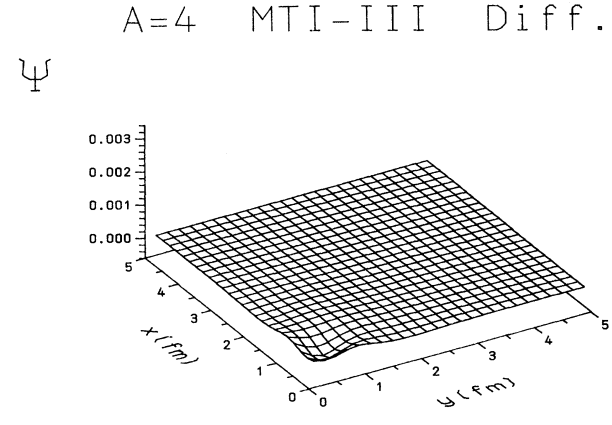

FIG. 22. Difference between the IDEA and SIDE for the exact four-body wave-function component ψ for the MT-I/III potential, displayed in terms of the coordinates x and y.

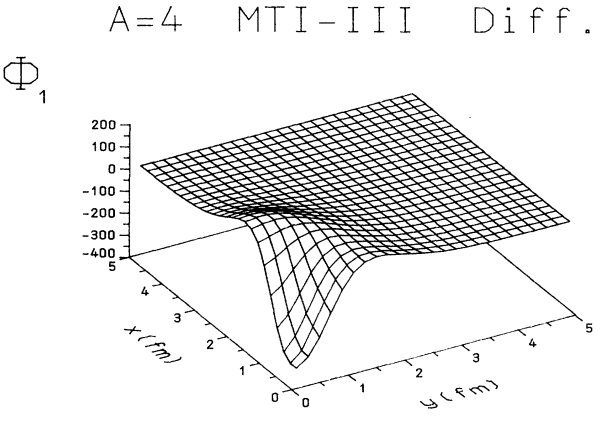

FIG. 24. Difference between the IDEA and SIDE for the exact four-body wave-function component ϕ_1 for the MT-I/III potential, displayed in terms of the coordinates x and y. Note that the values of the z axis are enlarged by a factor of 10^6.

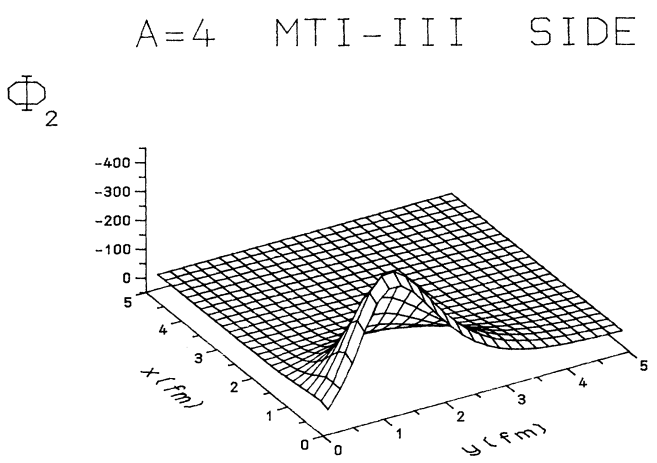

FIG. 25. Exact four-body wave-function component ϕ_2 for the MT-I/III potential in the case of the SIDE, displayed in terms of the coordinates x and y. Note that the values of the z axis are enlarged by a factor of 10.[6]

considerable difference in ϕ_1 for these cases, reflecting the corresponding situation for the Faddeev amplitudes.

Our results confirm the conclusion of Friar *et al.*[4] that the Faddeev amplitudes are relatively smooth compared to the Schrödinger wave-function components for the trinucleon and show that this remains true even for the modified Faddeev components of the IDEA, which incorporate the hypercentral potential in their definition. Our simplified ^{4}He Faddeev amplitudes and Schrödinger wave functions (restricted to two-particle correlations only) show a similar behavior.

IV. CONCLUSIONS

We have shown using the MT-V and MT-I/III potentials that the Faddeev components for S-wave projected potentials (SIDE), or for fully local potentials in the approximation where we incorporate the hypercentral potential $V_0(r)$ in the definition of the modified Faddeev components (IDEA), are quite similar as far as their fully symmetric S-state components are concerned, but that their mixed symmetric S'-state components are rather different. In our integro-differential equation approach, which only includes two-particle correlations for $A \geq 4$, the coupled system of integro-differential equations for the Faddeev-type components of the four-nucleon ground state retains a three-body-like character and depends only on two variables as for the trinucleon system. These four-body Faddeev amplitudes can therefore be directly compared to the three-body Faddeev amplitudes. We have already previously seen that very good results are obtained in this way for the four-nucleon binding energy and even for 16-fermion systems. Here we show that the four-body Faddeev components defined in this way are similar in shape to those of the trinucleon system both in the SIDE and IDEA, in particular for the fully symmetric S state. Although discrepancies occur between the shapes of the amplitudes $\psi_{ij}^{s'}$ for $A=3$ and 4, these are not large and are smaller than those between the SIDE and IDEA occurring for either $A=3$ or 4. Of course, the normalizations of these amplitudes going from $A=3$ to 4 are quite different (there are six four-body Faddeev amplitudes for $A=4$ and only three for $A=3$). The differences between the $\psi_{ij}^{s'}$ for four nucleons in the SIDE and IDEA are quite similar to the corresponding ones in the trinucleon. Our integro-differential equation approach therefore has the nice feature that it allows us to investigate the A dependence of the Faddeev amplitudes and their sensitivity to the inclusion of the hypercentral potential in their definition.

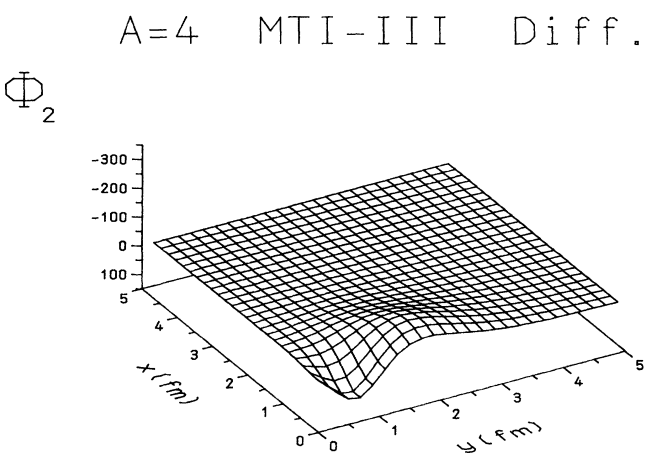

FIG. 26. Difference between the IDEA and SIDE for the exact four-body wave-function component ϕ_2 for the MT-I/III potential, displayed in terms of the coordinates x and y. Note that the values of the z axis are enlarged by a factor of 10^6.

Another important point which needed further investigation is how accurate are the wave functions obtained in the adiabatic approximation. Previous work has already confirmed that the extreme and uncoupled adiabatic approximations produce good estimates for the binding energies obtained by the exact solution of the integro-differential equations (by means of an empirical interpolation formula). Our present results confirm that already the Faddeev-type components calculated in the EAA (which is less accurate than the UAA) are generally in good agreement with the exact ones, particularly for fully symmetric S states, but also to a lesser extent for the S' states of mixed symmetry. In accordance with the known fact that the adiabatic approximations improve with increasing A, we find the greatest discrepancy for S' states and $A=3$. Our general conclusion is, however, that the adiabatic approximations are surprisingly accurate not only for the binding energies, but to the same degree of accuracy also for the Faddeev amplitudes, in contrast to the corresponding behavior of variational binding energies and wave functions.

To conclude, the most interesting feature of our three-dimensional graphical plots for the Faddeev amplitudes is the very high degree of similarity between their shapes for three- and four-nucleon ground states.

We have also presented the different components ψ, ϕ_1, and ϕ_2 of the Schrödinger wave function for the three- and four-nucleon ground states for the MT-I/III poten-

tial and confirmed that their behavior is as one would have expected from the fact that they are obtained by adding the respective Faddeev-type components.

Finally, we confirm the validity of the conclusion of Friar *et al.*[4] for the trinucleon that the Schrödinger wave function has more structure (i.e., is less smooth) than the Faddeev amplitude, for both the SIDE and IDEA. Going beyond the trinucleon wave function to four nucleons, we have demonstrated that, when only two-particle correlations are taken into consideration, this is also true for the Faddeev amplitudes and Schrödinger wave functions in that case.

ACKNOWLEDGMENTS

This work was partly supported by the Deutsche Forschungsgemeinschaft. One of us (H.E.) especially wants to express his gratitude to the Deutsche Forschungsgemeinschaft for providing financial support for a guest professorship at the University of Bonn and to Prof. W. Sandhas and his collaborators at the Physikalisches Institut of this University for their warm hospitality.

[1]W. Oehm, S. A. Sofianos, H. Fiedeldey, and M. Fabre de la Ripelle, Physikalisches Institut Report No. Bonn-ME-90-01 (ISSN-0936-2797); Phys. Rev. C (to be published).

[2]M. Fabre de la Ripelle, H. Fiedeldey, and S. A. Sofianos, Phys. Rev. C **38**, 449 (1988).

[3]M. Fabre de la Ripelle, H. Fiedeldey, and S. A. Sofianos, Few-Body Syst. **6**, 157 (1989).

[4]J. L. Friar, B. F. Gibson, and G. L. Payne, Z. Phys. A **301**, 309 (1981); see also G. L. Payne, J. L. Friar, B. F. Gibson, and I. R. Afnan, Phys. Rev. C **22**, 823 (1980); G. L. Payne, J. L. Friar, and B. F. Gibson, *ibid.* **22**, 832 (1980).

[5]M. Fabre de la Ripelle, Few-Body Syst. **1**, 181 (1986).

[6]S. P. Merkuriev and S. L. Yakovlev, Yad. Fiz. **39**, 1580 (1990) [Sov. J. Nucl. Phys. **39**, 1002 (1984)].

[7]S. P. Merkuriev, S. L. Yakovlev, and C. Gignoux, Nucl. Phys. **A431**, 125 (1984).

[8]J. L. Friar, Few-Body Syst. Suppl. **2**, 51 (1987).

[9]R. A. Malfliet and J. A. Tjon, Nucl. Phys. **A127**, 161 (1969).

[10]S. A. Sofianos, H. Fiedeldey, and M. Fabre de la Ripelle, Phys. Lett. B **205**, 163 (1988).

[11]S. A. Sofianos, H. Fiedeldey, H. Haberzettl, and W. Sandhas, Phys. Rev. C **26**, 228 (1982).

[12]J. A. Tjon, Phys. Lett. **56B**, 217 (1975).

[13]P. M. Prenter, *Splines and Variational Methods* (Wiley, New York, 1975).